


RESEARCH

Open Access



Alzheimer's disease brain contains tau fractions with differential prion-like activities

Longfei Li^{1,2†}, Ruirui Shi^{1,2†}, Jianlan Gu^{1,2}, Yunn Chyn Tung¹, Yan Zhou^{1,2}, Dingwei Zhou², Ruozhen Wu^{1,2}, Dandan Chu^{1,2}, Nana Jin^{1,2}, Kevin Deng¹, Jiawei Xu², Cheng-Xin Gong¹, Khalid Iqbal¹ and Fei Liu^{1*} 

Abstract

Neurofibrillary tangles (NFTs) made of abnormally hyperphosphorylated tau are a hallmark of Alzheimer's disease (AD) and related tauopathies. Regional distribution of NFTs is associated with the progression of the disease and has been proposed to be a result of prion-like propagation of misfolded tau. Tau in AD brain is heterogenous and presents in various forms. In the present study, we prepared different tau fractions by sedimentation combined with sarkosyl solubility from AD brains and analyzed their biochemical and pathological properties. We found that tau in oligomeric fraction (O-tau), sarkosyl-insoluble fractions 1 and 2 (SI₁-tau and SI₂-tau) and monomeric heat-stable fraction (HS-tau) showed differences in truncation, hyperphosphorylation, and resistance to proteinase K. O-tau, SI₁-tau, and SI₂-tau, but not HS-tau, were hyperphosphorylated at multiple sites and contained SDS- and β -mercaptoethanol-resistant high molecular weight aggregates, which lacked the N-terminal portion of tau. O-tau and SI₂-tau displayed more truncation and less hyperphosphorylation than SI₁-tau. Resistance to proteinase K was increased from O-tau to SI₁-tau to SI₂-tau. O-tau and SI₁-tau, but not SI₂-tau or HS-tau, captured tau from cell lysates and seeded tau aggregation in cultured cells. Heat treatment could not kill the prion-like activity of O-tau to capture normal tau. Hippocampal injection of O-tau into 18-month-old FVB mice induced significant tau aggregation in both ipsilateral and contralateral hippocampi, but SI₁-tau only induced tau pathology in the ipsilateral hippocampus, and SI₂-tau and HS-tau failed to induce any detectable tau aggregation. These findings suggest that O-tau and SI₁-tau have prion-like activities and may serve as seeds to recruit tau and template tau to aggregate, resulting in the propagation of tau pathology. Heterogeneity of tau pathology within AD brain results in different fractions with different biological and prion-like properties, which may pose a major challenge in targeting tau for development of effective therapeutic treatments.

Keywords: Alzheimer's disease, Tau pathology, Tau phosphorylation, Tau truncation, Prion-like seeding activity

Introduction

Alzheimer's disease (AD) is characterized pathologically by extracellular amyloid β (A β) plaques and intracellular neurofibrillary tangles (NFTs) composed of abnormally hyperphosphorylated tau. Tau lesion (pretangles, neuropil threads, and NFTs), but not A β plaque load, is

correlated with cognitive disturbances [2, 5, 23], suggesting a fundamental role of tau pathology in neurodegeneration of this disease.

In AD brain, tau pathology starts in the trans-entorhinal cortex, from where it spreads to limbic regions, followed by neocortical areas, according to the famous Braak stages [7, 8]. The distribution of NFTs associates with the progression of this disease [8, 23]. After examining the brains of younger cohorts and discovering NFTs in the locus ceruleus of a subset of individuals, Braak revised that subcortical nuclei may actually be the site of the initial seed for tau propagation [12].

*Correspondence: fei.liu@opwdd.ny.gov

[†]Longfei Li and Ruirui Shi contributed equally to this work

¹ Department of Neurochemistry, Inge Grundke-Iqbal Research Floor, New York State Institute for Basic Research in Developmental Disabilities, 1050 Forest Hill Road, Staten Island, NY 10314, USA

Full list of author information is available at the end of the article



Recently, tau tracer retention measured by positron emission tomography also showed similar stages [35, 51, 52]. Thus, tau pathology in AD brain may spread along neuroanatomical connections, which underlies the progression of AD.

The spatiotemporal spreading of tau pathology in AD was replicated recently in animal models. Clavaguera et al. injected brain extract from tau_{P301S} transgenic mice into the brain of wild-type tau-expressing mice and induced tau aggregation not only at the injection sites, but also in the anatomically connected brain regions in a time-dependent manner [13], leading to introduction of the concept of “propagation of tau pathology.” After this study, various mouse models were used to study the progressive propagation of tau pathology, including those using regional promoters, inoculation models, and viral models [1, 15, 16, 30, 32, 42, 47]. Tau pathology apparently radiates through the brain along synaptically connected pathways as the disease progresses.

As early as 1994, our group demonstrated that hyperphosphorylated cytosolic/oligomeric tau (AD p-tau) sequesters/captures normal tau in vitro to form filaments in a non-saturable manner [3], which was the first identification of prion-like activity of AD p-tau. Misfolded tau aggregates from brains of individuals with AD or tauopathies [6, 14, 30, 36] or from tau transgenic mouse brains [37] or generated in vitro [18, 27, 32, 50] are able to seed tau aggregation in cultured cells and in vivo. The seeding ability of tau from AD brains correlates positively with Braak stage and negatively with MMSE scores and precedes overt tau pathology [19]. In tau transgenic mice, tau seeds predict the spread of disease by appearing in brain regions prior to the appearance of any other pathological change [29]. Thus, the prion-like seeding activity of pathological tau may indicate the progression of tau pathology in AD.

Tau presents in different forms in AD brain [39], but its prion-like seeding activity is not well documented. By combining Kopke’s and Guo’s protocols [28, 39], we separated various tau fractions from AD brains, oligomeric fraction (O-tau), and sarkosyl-insoluble fractions 1 and 2 (SI₁-tau and SI₂-tau), and heat-stable tau (HS-tau) (Fig. 1), by sedimentation in sarkosyl buffer and assessed their seeding activity by using new methods we recently developed [26]. We found that different AD tau fractions displayed different properties in truncation, hyperphosphorylation, resistance to proteinase K, capturing normal tau in vitro and seeding tau aggregation in cultured cells and in vivo. O-tau and loose aggregates of tau in SI₁-fraction showed prion-like activity, which is inert in compacted aggregates of tau in SI₂-fraction and monomeric heat-stable tau.

Materials and methods

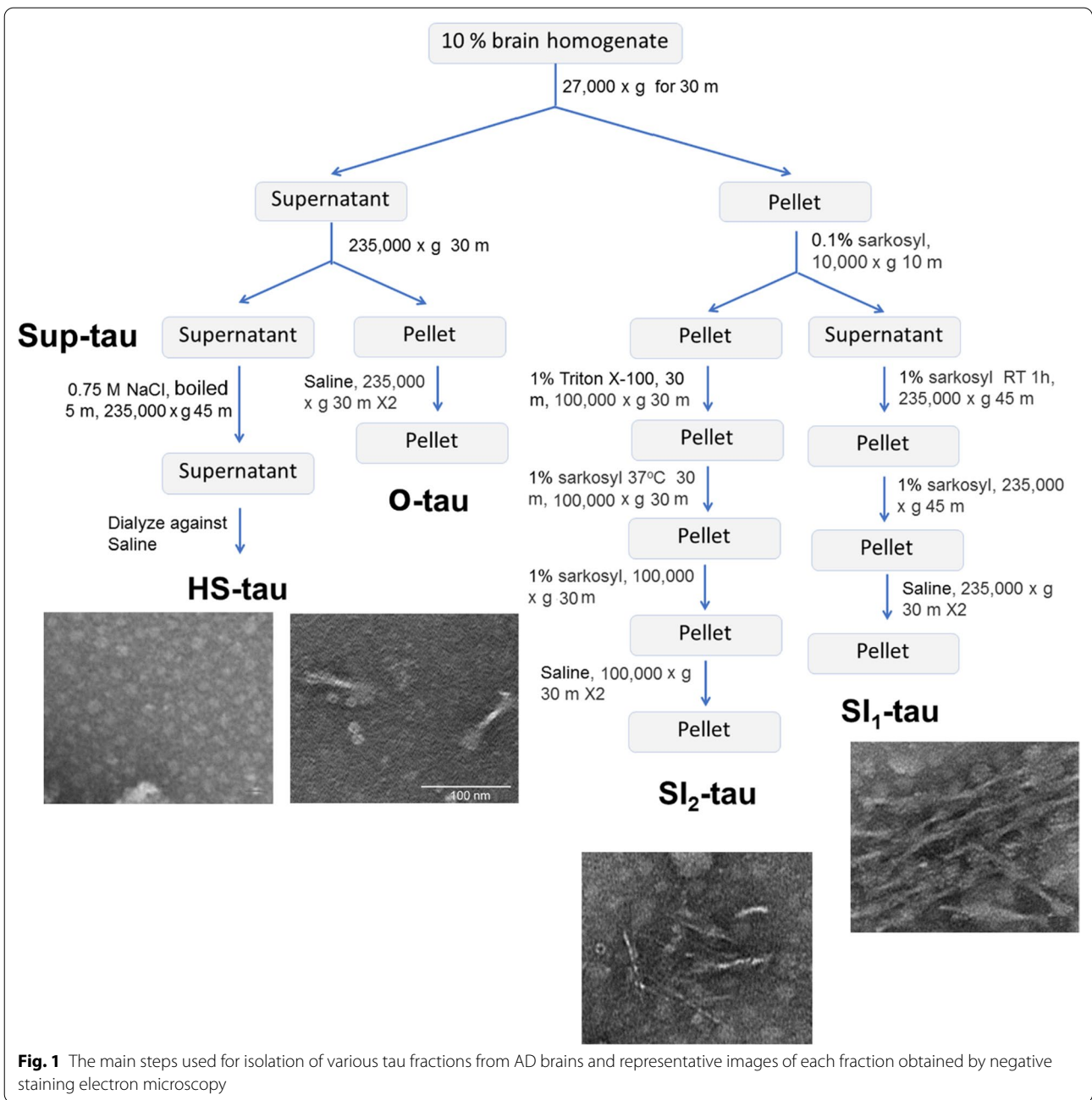
Isolation of various tau fractions from AD brain

Frozen brain tissue samples from autopsied and histopathologically confirmed AD cases with Braak Stages V and VI were obtained from the Brain Tissue Resource Center, McLean Hospital, Belmont, MA, USA. The use of autopsied frozen human brain tissue was in accordance with the National Institutes of Health guidelines and was exempted by the Institutional Review Board (IRB) of the New York State Institute for Basic Research in Developmental Disabilities because “the research does not involve intervention or interaction with the individuals” nor “is the information individually identifiable”.

Tau fractions were isolated from autopsied and frozen AD cerebral cortex by a combination of the protocols described by Kopke and by Guo [28, 39]. Briefly (Fig. 1), 10% brain homogenate prepared in homogenization buffer (20 mM Tris-HCl, pH 8.0, 0.32 M sucrose, 10 mM β-mercaptoethanol (β-ME), 5 mM MgSO₄, 1 mM EDTA, 10 mM glycerophosphate, 1 mM Na₃VO₄, 50 mM NaF, 2 mM benzamidine, 1 mM 4-(2-aminoethyl) benzenesulfonyl fluoride hydrochloride (AEBSF), and 10 μg/ml each of aprotinin, leupeptin, and pepstatin) was centrifuged at 27,000×g for 30 min. The pellet was saved for sarkosyl-insoluble tau (SI-tau) preparation. The supernatant was further centrifuged at 235,000×g for 30 min, and the resulting pellet, i.e., oligomeric tau-enriched fraction (O-tau), was collected and washed twice with saline and then resuspended in saline (Fig. 1). The supernatant, Sup-tau (Fig. 1), was used for HS-tau preparation.

Sarkosyl-insoluble aggregated tau preparation: The pellet from the 27,000×g centrifugation above was homogenized in the homogenization buffer containing 0.1% sarkosyl and centrifuged at 10,000×g for 10 min. The supernatant was adjusted to 1% sarkosyl, incubated for 1 h at room temperature (RT), and centrifuged at 235,000×g for 45 min. The pellet was washed once with 1% sarkosyl-homogenization buffer and washed twice with saline to obtain SI₁-tau (Fig. 1). The pellet from the 10,000×g centrifugation above was incubated with 1% Triton X-100 in homogenization buffer for 30 min at RT and centrifuged for 1 h at 100,000×g. The resulting pellet was incubated in 1% sarkosyl in homogenization buffer for 1 h at RT and centrifuged at 100,000×g for 45 min. The resulting pellet was washed once with 1% sarkosyl in homogenization buffer and twice with saline and collected as SI₂-tau (Fig. 1).

HS-tau preparation: The supernatant from the 235,000×g centrifugation above was adjusted to 0.75 M NaCl and 10 mM β-ME, heated for 5 min at 100 °C, and centrifuged at 235,000×g for 45 min. The resulting supernatant was dialyzed against saline; the tau in this pool was termed HS-tau (Fig. 1).



The tau preparations derived from AD brain described above were probe-sonicated for 5 min at 20% power and stored at -80°C until use.

Negative staining electron microscopy

Various tau fractions were placed on 300 meshed carbon-coated copper grids for 1 min, stained with one drop of 2% Phosphotungstic acid for 1 min, and visualized with Hitachi HT7700 transmission electron microscope.

Cell culture and transfection

HEK-293FT cells and HeLa cells were maintained in Dulbecco's modified Eagle's medium (DMEM) supplemented with 10% fetal bovine serum (FBS) (ThermoFisher Scientific, Waltham, MA, USA) at 37°C (5% CO_2). Transfections were performed with FuGENE HD (Promega, Madison, WI, USA) according to the manufacturer's instructions.

Western blots and immuno-dot blots

Samples were denatured by boiling in Laemmli buffer for 5 min. Protein concentration was measured using the Pierce™ 660 nm Protein Assay Kit (ThermoFisher Scientific). Samples were subjected to SDS-PAGE and transferred onto polyvinylidene fluoride membrane (Millipore Sigma, Burlington, MA, USA). The membrane was subsequently blocked with 5% fat-free milk-TBS (Tris-buffered saline) for 30 min, incubated with primary antibodies (Table 1) in 5% fat-free milk-TBS overnight, washed with TBST (TBS containing 0.05% Tween 20), incubated with peroxidase (HRP)-conjugated secondary antibodies (Jackson ImmunoResearch Laboratories, West Grove, PA, USA), washed with TBST, incubated with the ECL Western Blotting Substrate (ThermoFisher Scientific) and exposed to HyBlot CL® autoradiography film (Denville Scientific Inc., Holliston, MA, USA). Specific immunosignal was quantified by using the Multi Gauge software V3.0 from Fuji Film (Minato, Tokyo, Japan).

Tau level in samples was assayed by immuno-dot blots as described previously. Briefly, various amounts of a sample were applied onto nitrocellulose (NC) membrane (Schleicher and Schuell, Keene, NH, USA) at 5 µl per grid

of 7 × 7 mm in size. The blot was placed in a 37 °C oven for 1 h to allow the protein to bind to the membrane. Then, the membrane was processed as for Western blots described above by using a mixture of R134d and 92e pan tau antibodies as primary antibodies.

Proteolysis of AD tau fractions by proteinase K

AD tau fractions (2.5 mg/ml) were incubated with various concentration of proteinase K in 10 mM Tris-HCl, pH 7.4, for 10 min at RT. The reaction was stopped by boiling in Laemmli buffer for 5 min. Proteolyzed tau was analyzed by Western blots.

Tau capture/sequestration assay

Tau₁₅₁₋₃₉₁ tagged with hemagglutinin (HA) was overexpressed in HEK-293FT cells. The cells, 48 h after transfection, were lysed in phosphate-buffered saline (PBS) containing 50 mM NaF, 1 mM Na₃VO₄, 1 mM AEBSE, 5 mM benzamidine, and 10 µg/ml each of aprotinin, leupeptin, and pepstatin by probe sonication at 20% power for 2 min. The cell lysates were centrifuged for 10 min at 10,000×g. The extract containing HA-tau₁₅₁₋₃₉₁ was stored at – 80 °C until use.

Table 1 Antibodies used in this study

Antibody	Type	Specificity	Species	Source/reference (cat/lot)
43D	Mono-	Pan-tau (a.a. 6–18)	M	In house/Biolegend (816601)
92e	Poly-	Pan-tau	R	In house [40]
R134d	Poly-	Pan-tau	R	In house [40]
111e	Poly-	Pan-tau	R	In house [40]
113e	Poly-	Tau (a.a. 19–32)	R	In house [40]
HT7	Mono-	tau (a.a. 159–163)	M	ThermoFisher (MN10000/LK152163)
Tau5	Mono-	tau (a.a. 210–230)	M	Millipore (MAB361/1816394)
77G7	Mono-	tau (a.a. 244–368)	M	In house/Biolegend (816701)
RD3	Mono-	3R-tau	M	Millipore (05-803/JBC1863429)
RD4	Mono-	4R-tau	M	Millipore (05-804/2073108)
QCB23070	Poly-	Up-tau (S46)	R	Gong et al. [21]
Tau-1	Mono-	Up-tau (S199/202)	M	Dr. Lester I. Binder
AT8	Mono-	p-tau (S202/T205)	M	ThermoScientific (MN1020/PI205175)
Anti-pT205	Poly-	p-tau (T205)	R	Invitrogen (44738G/RD214239)
Anti-pS214	Poly-	p-tau (S214)	R	Invitrogen (44742G/0500B)
Anti-pT217	Poly-	p-tau (T217)	R	Invitrogen (44744/785771A)
AT180	Mono-	p-tau (T231)	M	Invitrogen (MN1040/SH2406086)
Anti-pS262	Poly-	p-tau (S262)	R	Invitrogen (44-750G/0204)
PHF1	Mono-	p-tau (S396/404)	M	Dr. Peter Davies
R145	Poly-	p-tau (S422)	R	In house [40]
Anti-GAPDH	Poly-	GAPDH	R	Sigma (G9545/015M4824V)
Anti-HA	Mono-	HA	M	Sigma (H9658/112M4841)
Anti-HA	Poly-	HA	R	Sigma (H6908/115M4872V)

Mono- monoclonal, *p-* phosphorylated, *up-* unphosphorylated, *Poly-* polyclonal, *M* mouse, *R* rabbit

Various amounts of AD tau fractions were dotted on nitrocellulose membrane and dried at 37 °C for 1 h. The membrane was blocked with 5% fat-free milk-TBS for 1 h and incubated with the above cell extract containing HA-tau₁₅₁₋₃₉₁ overnight. After washing with TBST, captured HA-tau₁₅₁₋₃₉₁ was detected by incubating with anti-HA in 5% milk-TBST and processed as described above for immuno-dot blots.

AD tau fractions seed tau aggregation in cultured cells

HEK-293FT cells were transfected with pCI/HA-tau₁₅₁₋₃₉₁ with FuGENE HD. Similar levels of tau in various AD tau fractions were mixed with Lipofectamine 2000 (3% in Opti-MEM) (ThermoFisher Scientific) in 50 µl for 20 min at RT and added to the cell cultures in 24-well plate after 6 h transfection. The cells were then lysed in RIPA buffer (50 mM Tris-HCl, pH 7.4, 150 mM NaCl, 1% NP-40, 0.5% sodium deoxycholate, and 0.1% SDS) containing 50 mM NaF, 1 mM Na₃VO₄, 1 mM AEBSE, 5 mM benzamide, and 10 µg/ml each of aprotinin, leupeptin, and pepstatin for 20 min on ice after 42 h treatment. The cell lysates were centrifuged at 130,000×*g* for 45 min, and the resulting pellet was washed with RIPA buffer. The supernatants were pooled together as RIPA-soluble fraction and the pellet contained RIPA-insoluble fraction. Levels of RIPA-insoluble and -soluble tau were analyzed by Western blots developed with anti-HA.

To visualize tau aggregates induced by various AD tau fractions in cells, HA-tau₁₅₁₋₃₉₁ was overexpressed in HeLa cells and treated with tau fractions for 42 h, as described above. The cells were then fixed for 15 min with 4% paraformaldehyde in phosphate buffer, washed with PBS, and treated with 0.3% Triton in PBS for 15 min at RT. After blocking with 5% newborn goat serum, 0.1% Triton X-100, and 0.05% Tween 20 in PBS for 30 min, the cells were incubated with anti-HA in blocking solution overnight at 4 °C, washed with PBS, and incubated with Alexa Fluor 488-conjugated-secondary antibody for 2 h at RT. After washing with PBS, the cells were mounted with ProLong™ Gold antifade reagent (ThermoFisher Scientific) and observed with a Nikon confocal microscope. The experiment was performed in triplicate wells and eight fields were photographed from each well of each group. Percentage of cells with aggregated tau was determined. Each experiment was repeated at least twice.

Tau pathology templated by AD tau fractions in vivo

Similar amounts of tau in O-tau, SI₁-tau, SI₂-tau, and HS-tau determined by immuno-dot blots with mixture of two polyclonal pan-tau antibodies (92e and R134d) were injected into the hippocampus unilaterally in 18-month-old male and female FVB mice. Mice were deeply anesthetized and transcardially perfused with saline followed

by buffered 4% paraformaldehyde 3 months after tau injection. Brain was post-fixed in the same fixation buffer overnight at 4 °C and dehydrated in buffered 30% sucrose solution. Brain was then cut into 40-µm serial coronal sections by using a freezing microtome, and the sections were collected in a 12-well plate containing antifreeze solution (30% glycerol and 30% ethylene glycol in 40% PBS) in sequence, and the free-floating sections were preserved in antifreeze solution at -20 °C before immunohistochemical staining.

Immunofluorescent staining

Brain sections from one well of a 12-well plate per mouse were washed with PBS and treated with 0.3% Triton in PBS for 15 min at RT. After blocking with 5% newborn goat serum, 0.1% Triton X-100, and 0.05% Tween 20 in PBS for 30 min, the sections were incubated with AT8 antibody in blocking solution overnight at 4 °C, washed with PBS, and incubated with Alexa 555-conjugated-second antibody for 2 h. Hoechst dye was used to stain nuclei. After washing with PBS, sections were mounted on microscope slides, air-dried, mounted with ProLong™ Gold antifade reagent (ThermoFisher Scientific), and set under a coverslip before imaging using a Leica TCS SP5 confocal microscope. For quantification, average AT8-positive neurons in contralateral and ipsilateral hippocampi were counted from three brain sections per mouse.

Statistical analysis

The GraphPad Prism 6 software was used for statistical analysis. Results were analyzed by one-way ANOVA followed with Tukey's multiple comparisons test or by two-way ANOVA followed by Sidak's multiple comparisons test for multiple-group analysis.

Results

AD tau fractions are truncated differentially

Tau in AD brain appears in various pools and in monomeric, oligomeric, and filamentous forms [39]. In addition to aggregated tau, AD brain also expresses similar levels of normal tau [38], which is heat-stable [17]. Aggregated tau is sarkosyl-insoluble [22]. Normal tau and pathological tau can be separated by sedimentation. In the present study, by combining Kopke's and Guo's protocols [28, 39], we isolated various tau fractions—O-tau, SI₁-tau, SI₂-tau, and HS tau—from AD brains (Fig. 1). Negative staining microscopy showed paired helical filaments in fraction SI₁-tau, mostly straight filaments in SI₂-tau, short filaments in O-tau, and non-filament in HS-tau (Fig. 1).

It is widely believed that truncation of tau plays a critical role in tau pathogenesis [49, 54, 58]. To reveal

the truncation of various AD tau fractions, we isolated aggregated O-tau, SI₁-tau, and SI₂-tau from four AD cerebral cortices and analyzed tau protein patterns by using polyclonal and monoclonal pan-tau antibodies to various regions of the protein (Fig. 2a). HS-tau from one AD brain was used as a reference. In general, we found SDS- and β-ME-resistant high-molecular weight-tau (HMW-tau) in O-tau, SI₁-tau, and SI₂-tau detected by R134d, 92e, and 111e (Fig. 2b). Heat treatment is known to remove aggregated tau [48]. We found no detectable HMW-tau in HS fraction (Fig. 2b). Compared with blots developed with antibodies R134d and 92e, a lesser amount of tau in SI₂ fraction was detected with antibody 111e (Fig. 2b).

To determine tau truncations, O-tau, SI₁-tau, SI₂-tau, and HS-tau were analyzed by Western blots developed with a battery of tau antibodies targeting specific epitopes (Fig. 2a). Consistently, SDS- and β-ME-resistant HMW-tau was seen in O-tau, SI₁-tau, and SI₂-tau but not in HS-tau (Fig. 2d). HMW-tau was detected by Tau5, 77G7, RD3, RD4, and Tau46, but was not, or only weakly, stained by N-terminal antibodies 43D, 113e, and HT7 (Fig. 2d), suggesting that it is truncated at the N-terminus. Immunoactivities of the N-terminal antibodies 43D, 113e, and HT7 were less in O-tau and SI₂-tau than in SI₁-tau (Fig. 2d, e). Tau5 immunoactivity was slightly higher in O-tau and SI₁-tau than in SI₂-tau (Fig. 2d, e). Interestingly, immunoactivities of three antibodies against the microtubule-binding repeats, 77G7, RD3 and RD4, were similarly decreased from O-tau, SI₁-tau to SI₂-tau (Fig. 2d, e), but 77G7 revealed strong immunoactivity toward O-tau, SI₁-tau, and SI₂-tau (Fig. 2d, e). Compared with SI₁-tau, a lower level of tau in O- and SI₂-fractions was detected by Tau46 (Fig. 2d, e). Taken together, these results suggest that AD tau fractions are truncated differentially. O-tau and SI₂-tau are truncated more at both N- and C-termini, compared with SI₁-tau.

AD tau fractions are hyperphosphorylated differentially

Tau is hyperphosphorylated and aggregated into NFTs in AD and related tauopathies [24, 25, 33, 41]. To determine tau hyperphosphorylation, four AD tau fractions were subjected to Western blots developed with site-specific and phosphorylation-dependent tau antibodies. Consistently, we found HMW-tau in O-tau, SI₁-tau, and SI₂-tau, but not in HS-tau. HMW-tau was detected by all phospho-tau antibodies (Fig. 3a). O-tau, SI₁-tau, and

SI₂-tau were hyperphosphorylated at Thr205, Thr212, Thr217, Ser231, Ser262, Ser396/404, and Ser422, but HS-tau was not, or only a little, phosphorylated at these sites (Fig. 3a, b). However, HS-tau was phosphorylated at Ser199 and Ser214 (Fig. 3a, b). Thus, O-, SI₁-, and SI₂-tau fractions, but not HS-tau, are hyperphosphorylated at multiple sites. The SDS- and β-ME-resistant HMW-tau is hyperphosphorylated.

O-tau and SI₂-tau showed similar phosphorylation levels, but both were less phosphorylated than SI₁-tau at Ser199, Thr205, Thr212, Ser214, Thr217, and Ser422 (Fig. 3a, b). O-tau and SI₁-tau were phosphorylated similarly, but SI₂-tau was less phosphorylated at Ser231 and Ser262, the sites in, or close to, microtubule-binding repeats (Fig. 3a, b). Similar phosphorylation levels of tau were observed in three AD tau fractions at Ser396/404 (Fig. 3a, b). Thus, these results suggest that O-tau, SI₁-tau, and SI₂-tau are hyperphosphorylated differentially. SI₁-tau may be more hyperphosphorylated than O-tau and SI₂-tau at most phosphorylation sites.

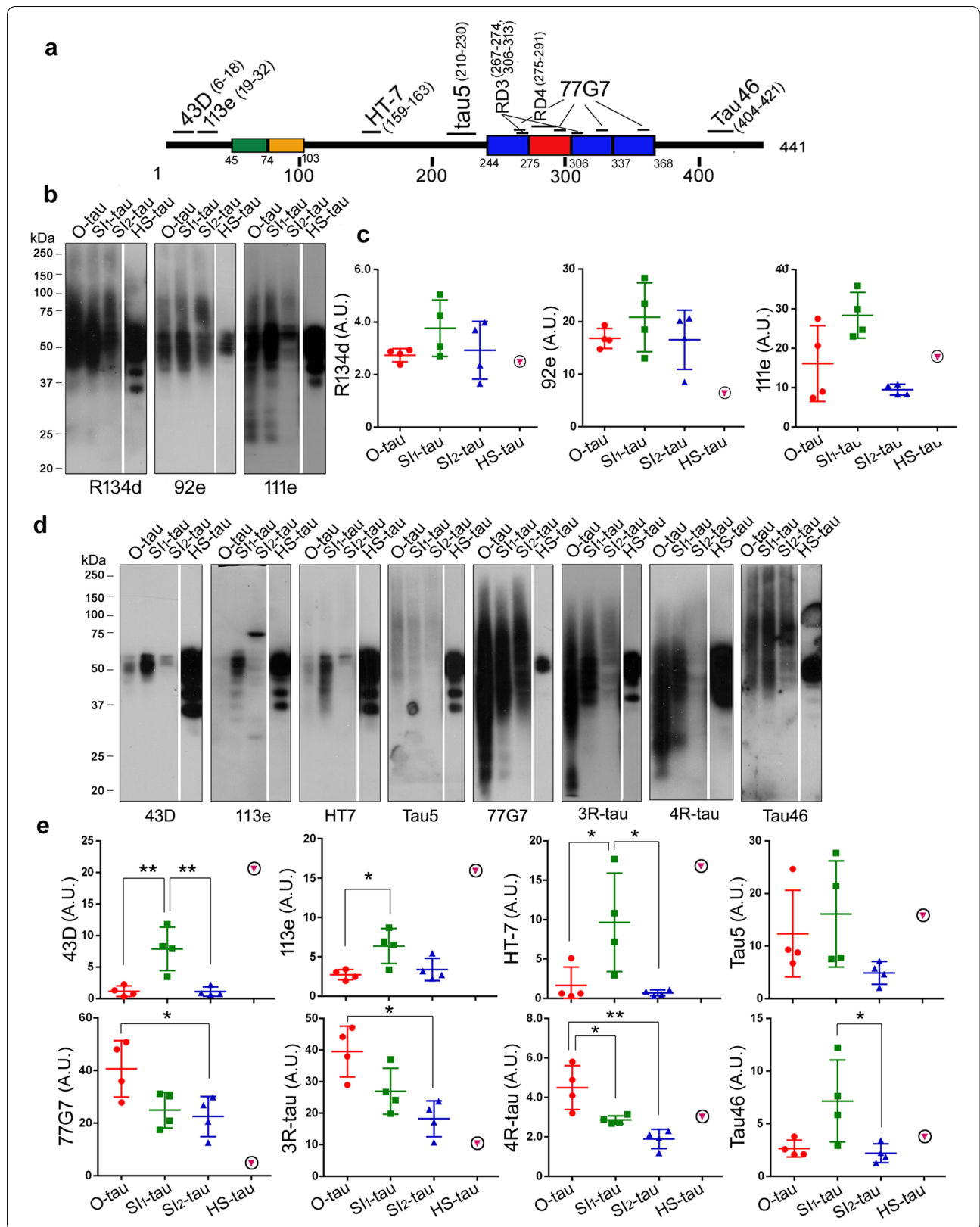
We also analyzed un-phosphorylated tau in these AD tau fractions by Western blots developed with antibodies to un-phosphorylated tau: Ser46 (Up-Ser46) and Tau-1 (Up-Ser195-202). We found no or very little un-phosphorylated tau at Ser46 and at Ser195-202 (Tau-1) in O-tau, SI₁-tau, and SI₂-tau, but marked levels in HS-tau (Fig. 3c, d). Moreover, SI₁-tau contained more un-phosphorylated tau than O-tau and SI₂-tau (Fig. 3c, d). These results showed that O-tau, SI₁-tau, and SI₂-tau are hyperphosphorylated, and HS-tau is less phosphorylated, at Ser46 and tau-1 sites. In addition to hyperphosphorylated tau, a small fraction of SI₁-tau also is un-phosphorylated at Ser46 and tau-1 sites.

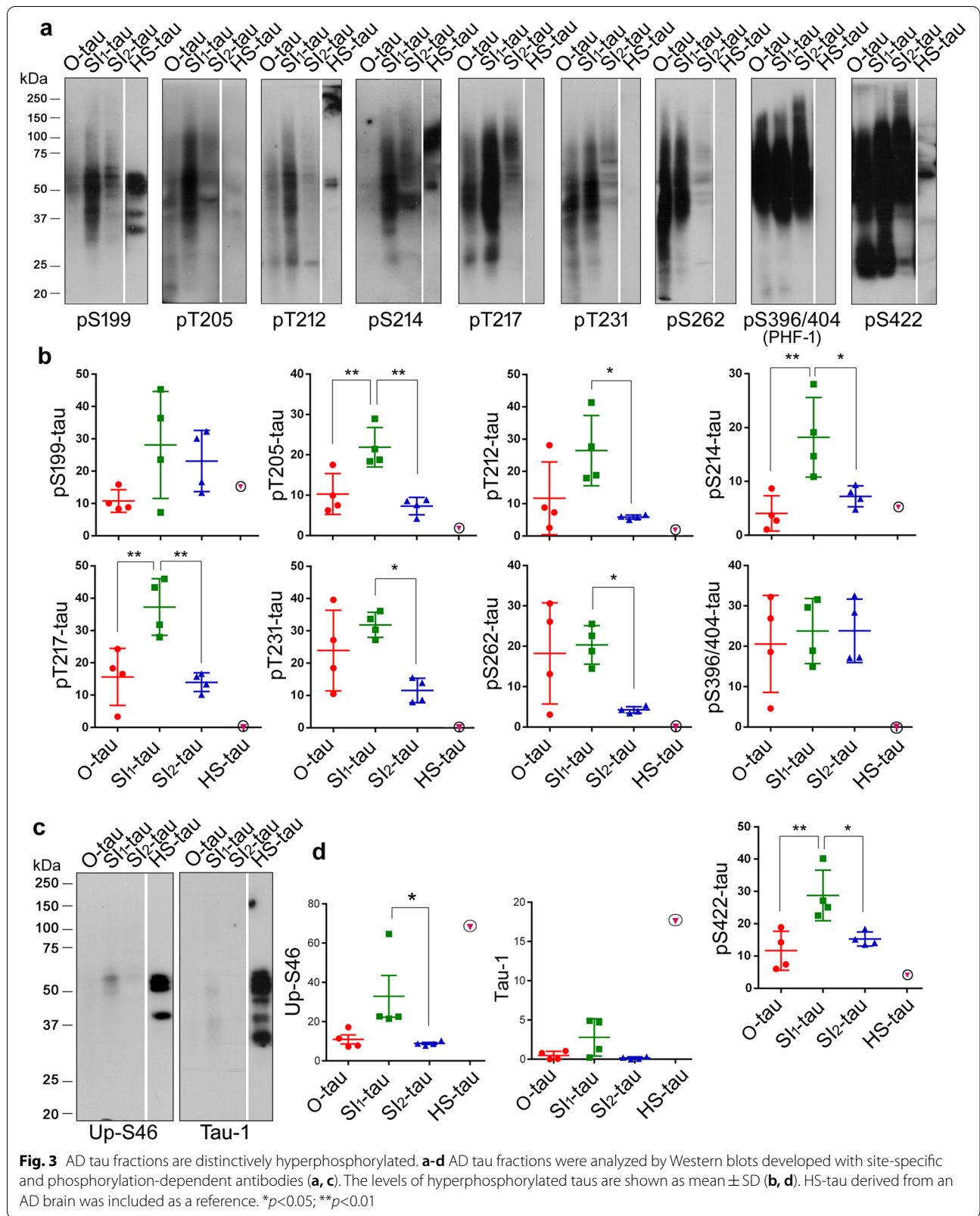
AD tau fractions are resistant to proteinase K differentially

It is well known that tau in NFT is resistant to proteinase K [56]. To determine the sensitivity of these AD tau fractions to proteinase K, we incubated them with various concentrations of proteinase K for 10 min at room temperature and analyzed the digestion products by Western blots developed with 77G7 and with a mixture of R134d and 92e. We found that proteinase K proteolyzed O-tau, SI₁-tau, and SI₂-tau to small-molecular weight products that immunoreacted with 77G7 (Fig. 4c), but weakly with R134d/92e (Fig. 4a) in a dose-dependent manner. The greater reductions of tau by

(See figure on next page.)

Fig. 2 AD tau fractions are truncated at different sites. **a**. Schematic showing the position of epitopes of various tau antibodies used to analyze tau truncation. **b-e** Western blots of O-tau, SI₁-tau, SI₂-tau, and HS-tau from AD brains developed with polyclonal pan-tau antibodies (R134d, 111e, and 92e) (**b**), or with epitope-specific antibodies (**d**). The levels of tau in the four pools determined by the individual antibody were quantified densitometrically and are presented as mean ± SD (**c, e**). **p*<0.05; ***p*<0.01. A.U., arbitrary units





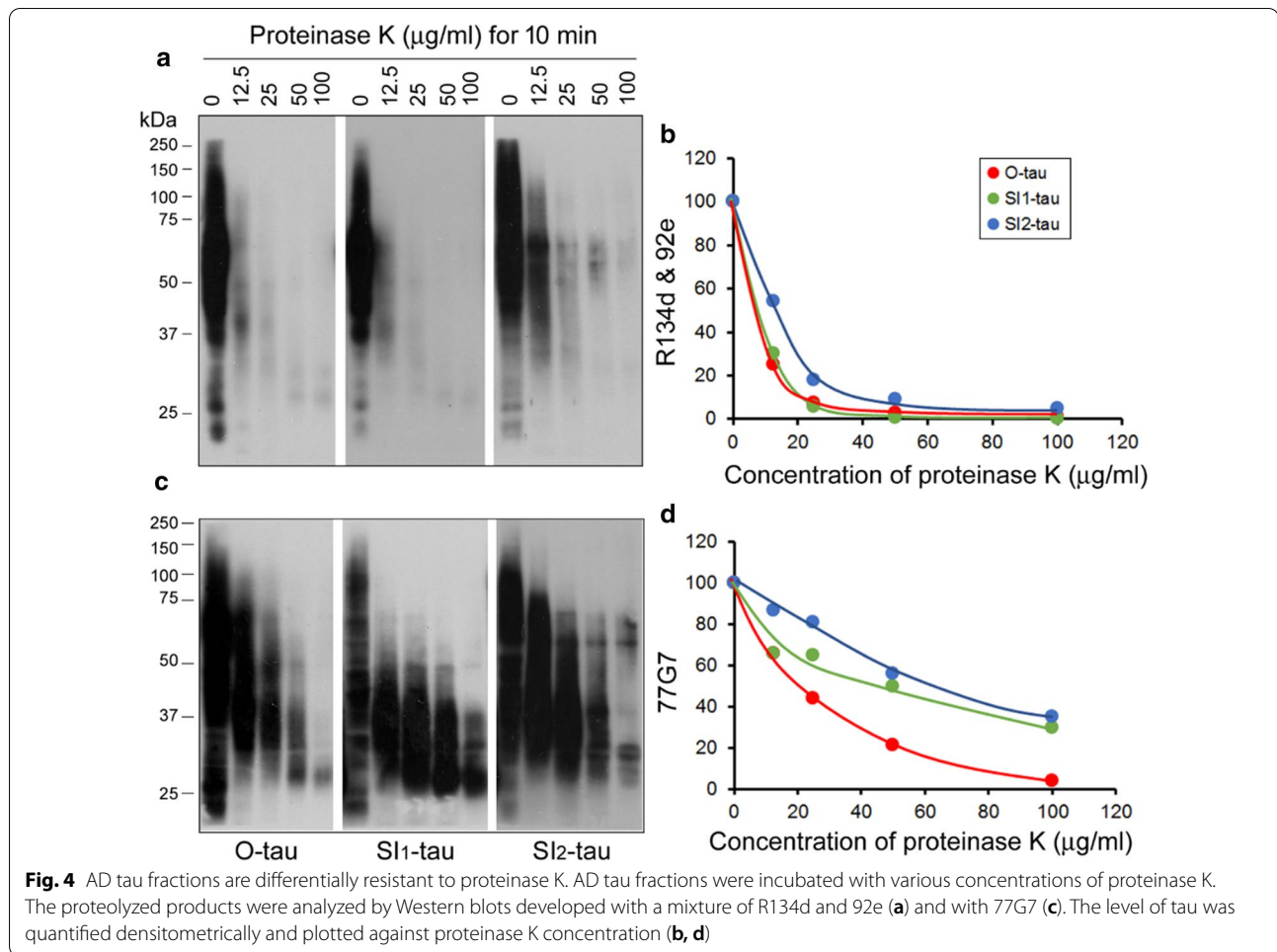


Fig. 4 AD tau fractions are differentially resistant to proteinase K. AD tau fractions were incubated with various concentrations of proteinase K. The proteolyzed products were analyzed by Western blots developed with a mixture of R134d and 92e (**a**) and with 77G7 (**c**). The level of tau was quantified densitometrically and plotted against proteinase K concentration (**b, d**)

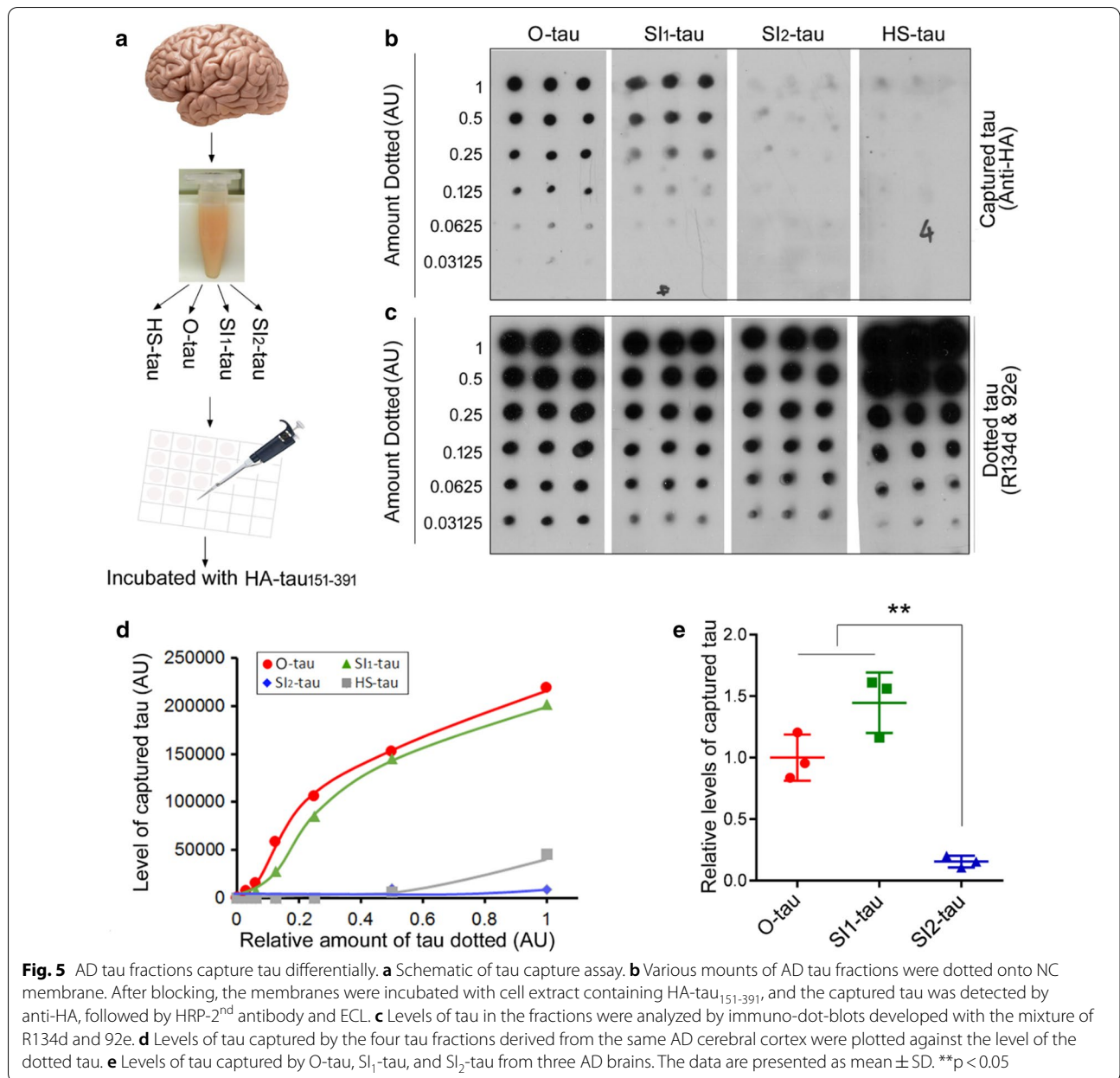
proteinase K were observed in the blots developed with R134d/92e than with 77G7 (Fig. 4b, d), suggesting that the microtubule-binding domain is relatively resistant to proteinase K. R134d/92e blot revealed that SI₂-tau was decreased less rapidly than O-tau and SI₁-tau (Fig. 4a, b), and 77G7 blots showed greater and faster reduction of O-tau than did SI₁-tau and SI₂-tau by proteinase K digestion (Fig. 4c, d). Both R134d/92e and 77G7 blots showed proteinase K-resistant 55- to 65-kDa tau in SI₂-tau, but not in other fractions. Taken together, these results suggest that the amount of resistance to proteinase K was O-tau < SI₁-tau < SI₂-tau.

AD tau fractions capture tau differentially

Aggregated and misfolded protein is able to recruit and to template the protein in normal conformation to the misfolded conformation, termed as the prion-like properties [20]. To determine the ability of AD tau fractions in recruiting tau, we performed overlay assay as reported recently [26]. We overexpressed tau₁₅₁₋₃₉₁ tagged with HA in HEK-293FT cells. The crude extract

of HEK-293/tau₁₅₁₋₃₉₁ was used in tau capture assay (Fig. 5a). Tau₁₅₁₋₃₉₁ comprises the β-sheet-forming core of the PHF structure. We dotted O-tau, SI₁-tau, SI₂-tau, and HS-tau with similar levels of tau on NC membrane. One membrane was incubated with the mixture of R134d and 92e to detect the levels of tau in the fractions. Another membrane was subjected to overlay assay. The membrane was incubated with HEK/tau₁₅₁₋₃₉₁ extract after blocking. The captured tau was analyzed by anti-HA followed by HRP-2nd antibody and ECL. The overlay assay revealed anti-HA immunoreactivity in the membrane dotted with O-tau and SI₁-tau, but not with SI₂-tau and HS-tau, in a dose-dependent manner (Fig. 5b, d), indicating capture of tau₁₅₁₋₃₉₁ by O-tau and SI₁-tau, but not SI₂-tau or HS-tau.

To further confirm capture of tau₁₅₁₋₃₉₁ by O-tau and SI₁-tau, but not by SI₂-tau, three sets of O-tau, SI₁-tau, and SI₂-tau from three AD brains were prepared and subjected to the overlay assay (Fig. 5a). Again, we found that O-tau and SI₁-tau were able, but SI₂-tau was



unable, to capture tau₁₅₁₋₃₉₁ from the cell extract consistently (Fig. 5e).

AD tau fractions seed tau aggregation in cultured cells differentially

Seeding tau aggregation by misfolded tau in cultured cells is the basis of prion-like activity. We recently reported deletion of the first 150 and the last 50 amino acid (a.a.) of tau enhanced its aggregation seeded by AD O-tau [26]. To determine the seeding activity of these AD tau fractions, we overexpressed HA-tau₁₅₁₋₃₉₁ in HeLa cells and treated the cells with O-tau, SI₁-tau,

SI₂-tau, or HS-tau containing similar tau levels for 42 h after 6 h transfection. The cells were immuno-stained with anti-HA, and the numbers of cells with aggregates were counted. No aggregated HA-tau₁₅₁₋₃₉₁ was observed in the cells without treatment with AD tau fractions (Fig. 6a, b). O-tau treatment induced ~25% cells with tau aggregates, and SI₁-tau induced ~15% cells with aggregation. Significantly fewer cells were induced to form aggregates by SI₂-tau, and no significant tau aggregates were formed by HS-tau (Fig. 6a, b). Thus, these results suggest the strongest seeding activity of O-tau. The seeding activity of AD tau fractions

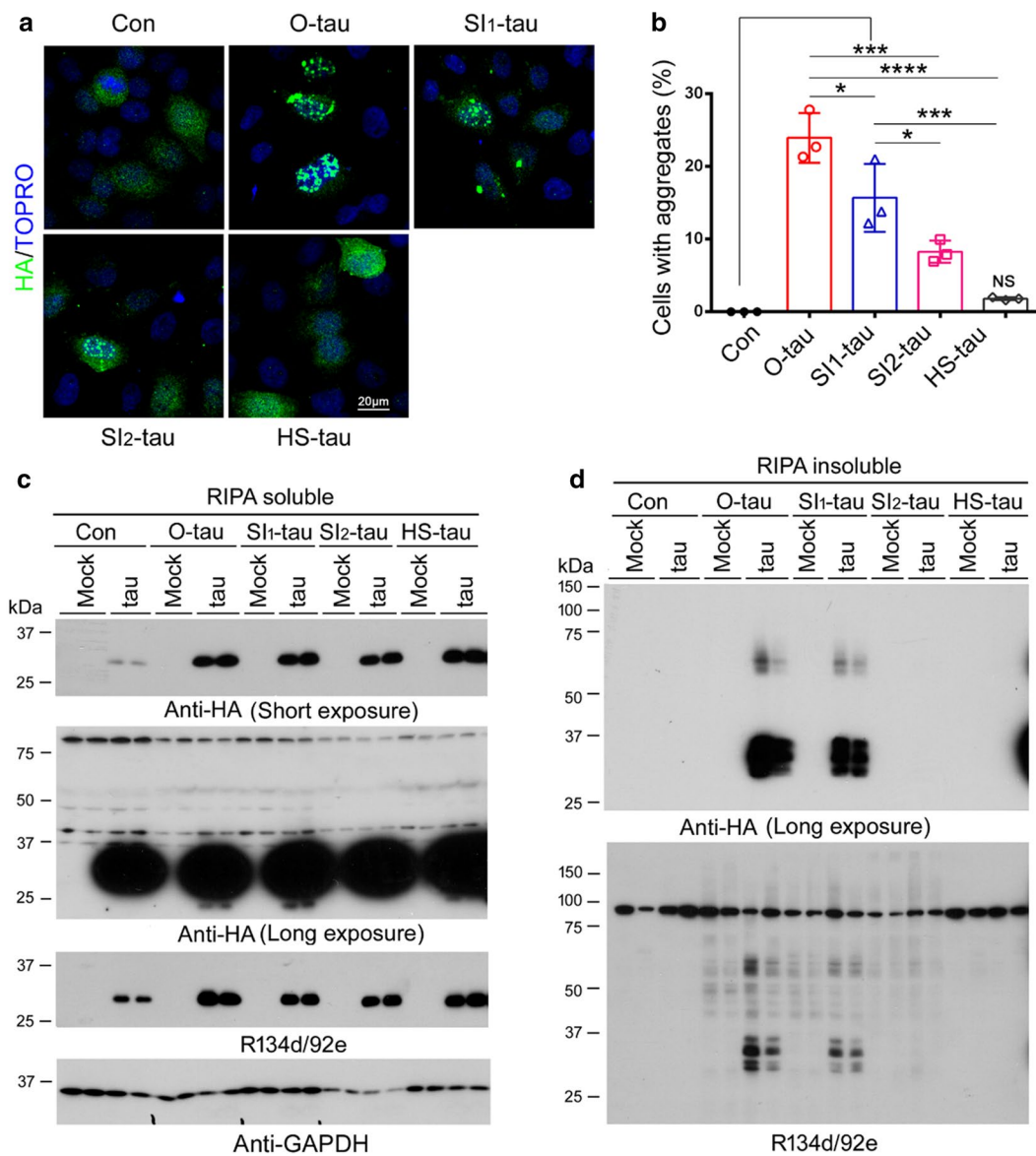


Fig. 6 AD tau fractions template tau aggregation in cultured cells distinctively. **a, b** HeLa cells were transfected with pCI/HA-tau₁₅₁₋₃₉₁ and treated with AD tau fractions containing similar tau levels. The cells were immunostained with anti-HA, followed by Alex488-Anti-mouse IgG. The numbers of cells with tau aggregation were counted. The data on the percentage of cells with aggregation are presented as mean ± SD. *p < 0.05, ***p < 0.001, ****p < 0.0001. **c, d** HEK-293FT/HA-tau₁₅₁₋₃₉₁ cells treated with AD tau fractions containing similar tau levels. The cells were lysed in RIPA buffer 42 h after treatment. RIPA-soluble (**c**) and -insoluble (**d**) taus were analyzed by Western blots developed with anti-HA and a mixture of R134d and 92e

was reduced gradually from O-tau, SI₁-tau, SI₂-tau, to HS-tau.

To analyze biochemically the tau aggregation induced by the AD tau fractions, we also lysed the cells with RIPA buffer and analyzed the levels of tau in RIPA-soluble and -insoluble fractions by Western blots developed with anti-HA and a mixture of R134d and 92e. Anti-HA blots revealed no soluble and insoluble tau in the mock

cells treated with AD tau fractions (Fig. 6c, d). The levels of RIPA-soluble tau₁₅₁₋₃₉₁ were found to be increased in cells treated with the tau fractions (Fig. 6c). A significant amount of RIPA-insoluble tau was found in HEK-293FT/HA-tau₁₅₁₋₃₉₁ cells treated with O-tau and SI₁-tau, but not in cells treated with SI₂-tau or HS-tau (Fig. 6d). We found only one 28-kDa band in RIPA-soluble fraction, but three major bands in RIPA-insoluble fraction

in cells treated with O-tau and SI₁-tau, which suggested hyperphosphorylation of RIPA-insoluble tau. In addition to ~28- to 32-kDa tau, we found 60- to 65-kDa SDS- and β-ME-resistant HMW-tau in RIPA-insoluble fractions in O-tau- and SI₁-tau-treated cells (Fig. 6d), but not in corresponding RIPA-soluble fractions (Fig. 6c). R134d/92e blots showed immunoactivity in tau strain-treated mock cells, but clearly more tau in HEK-293FT/HA-tau₁₅₁₋₃₉₁ cells treated with O-tau and SI₁-tau, compared with control treatment (Fig. 6d). Taken together, these results suggest that O-tau and SI₁-tau, but not SI₂-tau and HS-tau, have prion-like properties to seed tau aggregation in cultured cells.

Heat treatment does not passivate the prion-like activity of pathological tau

HS-tau derived from 235,000×g supernatant (Sup-tau) of brain homogenate by heat treatment (Fig. 1) did not show prion-like activities (Figs. 5, 6). HS-tau was less truncated and least phosphorylated. We found that both Sup-tau and HS-tau were almost similar in Western blots developed with polyclonal pan-tau antibodies (Fig. 7a), monoclonal antibodies against specific epitopes (Fig. 7b), and site-specific and phosphorylation-dependent tau antibodies (Fig. 7c), suggesting that heat treatment did not affect the truncation and phosphorylation of tau.

Next, we performed overlay assay as described above to compare the ability of Sup-tau with HS-tau to recruit tau. We found that consistently HS-tau could not capture tau, but Sup-tau was able to recruit tau from HEK-293FT/tau₁₅₁₋₃₉₁ cell extract (Fig. 7d, e), when even a smaller amount of tau in Sup-fraction was applied (Fig. 7d, e). These results suggest that either heat treatment inactivates tau's ability to bind to tau₁₅₁₋₃₉₁ or the Sup-tau might contain the small-size oligomers. It is well known that heat treatment removes aggregated tau [48]. Thus, unlike HS-tau, Sup-tau might contain small-size oligomeric tau.

We then studied whether heat treatment kills the prion-like activity of pathological tau. We dotted various amounts of O-tau on NC-membranes parallelly. One set of membranes was boiled in 50 mM Tris-HCl, 0.75 M NaCl, for 10 min to mimic heat treatment as the HS-tau preparation. Another membrane was incubated with the same buffer at RT as control treatment. Then, the membranes were overlaid with the HEK-293FT/tau₁₅₁₋₃₉₁ cell extract for tau capture assay or with a mixture of R134d and 92e for tau assay, as described above. We found that heat treatment caused a slight reduction of tau level (Fig. 7f, g). Similarly, a slightly lesser amount of tau was captured by heat-treated O-tau than by control O-tau (Fig. 7f, g), suggesting that the heat treatment did not affect the prion-like activity of O-tau.

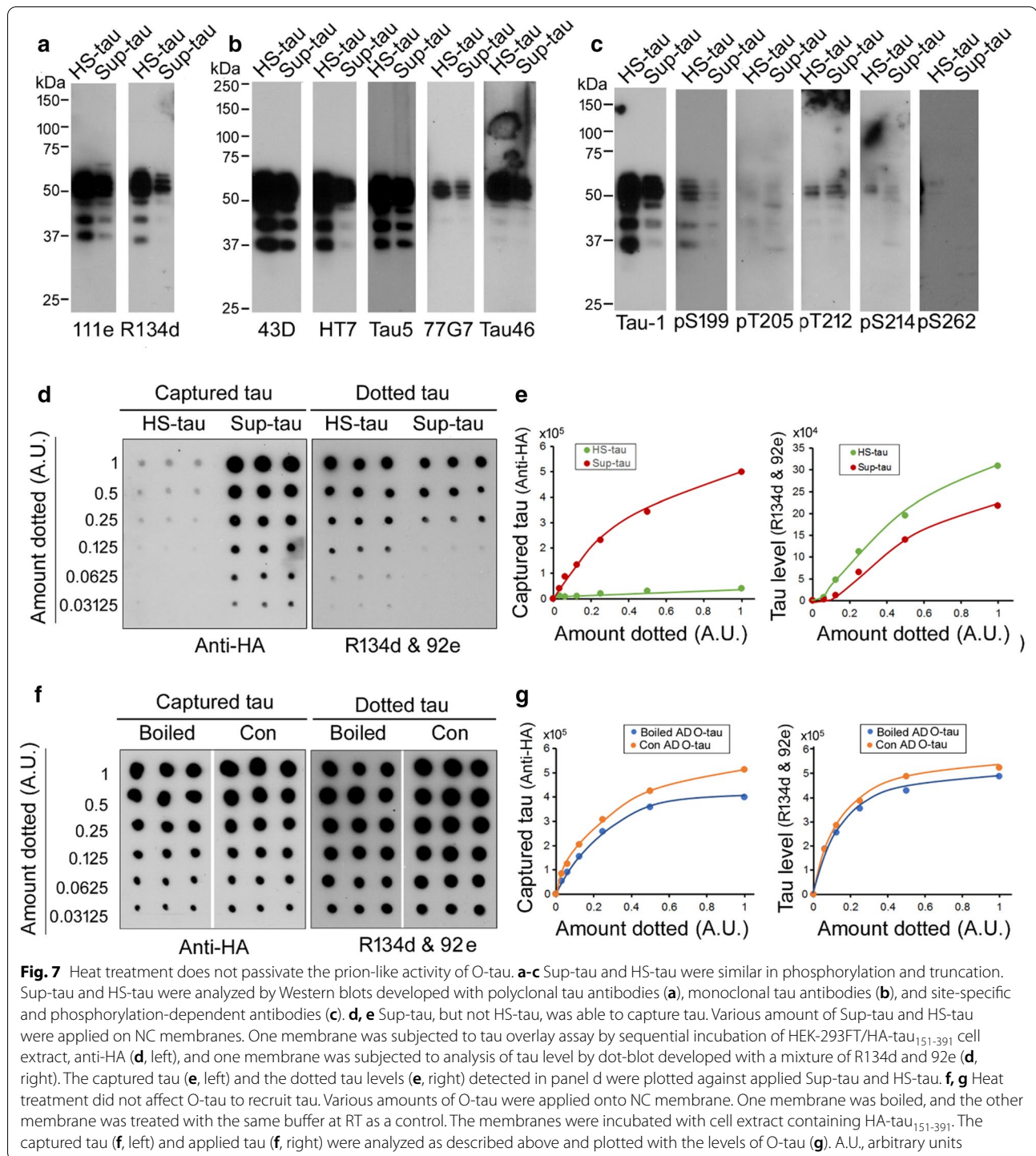
AD tau fractions induce tau pathology in vivo differentially

To determine the seeding activity of AD tau fractions in vivo, we injected the four AD tau fractions with similar tau levels into the hippocampus in 18-month-old FVB mice and analyzed tau pathology in ipsilateral and contralateral hippocampi by immunofluorescence staining with AT8 3 months after injection. We found many AT8-positive neurons in both the ipsilateral and contralateral CA1 (Fig. 8a) and the ipsilateral CA3 (Fig. 8b) of the hippocampi of mice injected with O-tau, and a few AT8-positive neurons in the ipsilateral CA1 (Fig. 8a) of SI₁-tau-injected mice. No obvious AT8 immunoactivity was observed in the ipsilateral and contralateral hippocampi of SI₂-tau- or HS-tau-injected mice. AT8 immunostaining was not detectable in the cortex of the mice injected with any of the four tau fractions. AT8 immunostaining was dramatically higher in both the ipsilateral and contralateral hippocampi injected with O-tau than in those injected with SI₁-tau, SI₂-tau, or HS-tau (Fig. 8c), suggesting that O-tau serves as potent seeds to induce tau pathology in vivo.

Discussion

Tau in AD brain exists in monomeric, oligomeric, and fibrillar forms. In the present study, we isolated from AD brain four fractions—O-tau, SI₁-tau, SI₂-tau, and HS-tau—and analyzed their biochemical and prion-like properties. We found that O-tau, SI₁-tau, and SI₂-tau, but not HS-tau, contained SDS- and reducing agent-resistant HMW-tau. O-tau and SI₂-tau revealed similar patterns of truncation and hyperphosphorylation. Compared to O-tau and SI₁-tau, SI₂-tau was more resistant to proteolysis by proteinase K. O-tau, SI₁-tau, but not SI₂-tau or HS-tau, captured/sequestered tau in vitro and templated tau aggregation in cultured cells. Heat treatment did not inactivate the prion-like activity of O-tau. O-tau induced tau pathology in the ipsilateral and contralateral hippocampi, SI₁-tau only induced it in the ipsilateral hippocampus, and SI₂-tau or HS-tau could not induce tau aggregation in the hippocampi of 18-month-old FVB wild-type mice, as determined 3 months after injection. These results suggest that tau in the four isolated fractions showed distinct biochemical and prion-like properties. O-tau and SI₂-tau showed similarities in hyperphosphorylation and truncation. Oligomeric O-tau and SI₁-tau in AD brain may serve as seeds to induce tau aggregation. Monomeric tau and SI₂-tau were inert in the prion-like properties, and they could not induce tau pathogenesis.

Tau is truncated at multiple sites in AD brain [49, 54]. Truncation may facilitate tau pathogenesis. We found in a parallel study that deletion of the first 150 or 230 a.a. and the last 50 a.a. enhanced tau's site-specific



hyperphosphorylation and self-aggregation as well as its binding to, and its aggregation seeded by, O-tau. tau₁₅₁₋₃₉₁, corresponding to the β -sheet-forming core of the PHF structure [46, 55], contains microtubule-binding repeats and showed the highest pathology-associated activities. The microtubule-binding repeats

of tau (tauRD) with P301S mutation have been used in HEK293-tau-biosensor cells for tau-seeding [57]. Tau₁₅₁₋₃₉₁ aggregates induced by O-tau were thioflavin T-positive and showed SDS- and β -ME-resistant HMW-tau in Western blots. By using RIPA buffer, aggregated tau was yielded in RIPA-insoluble fraction.

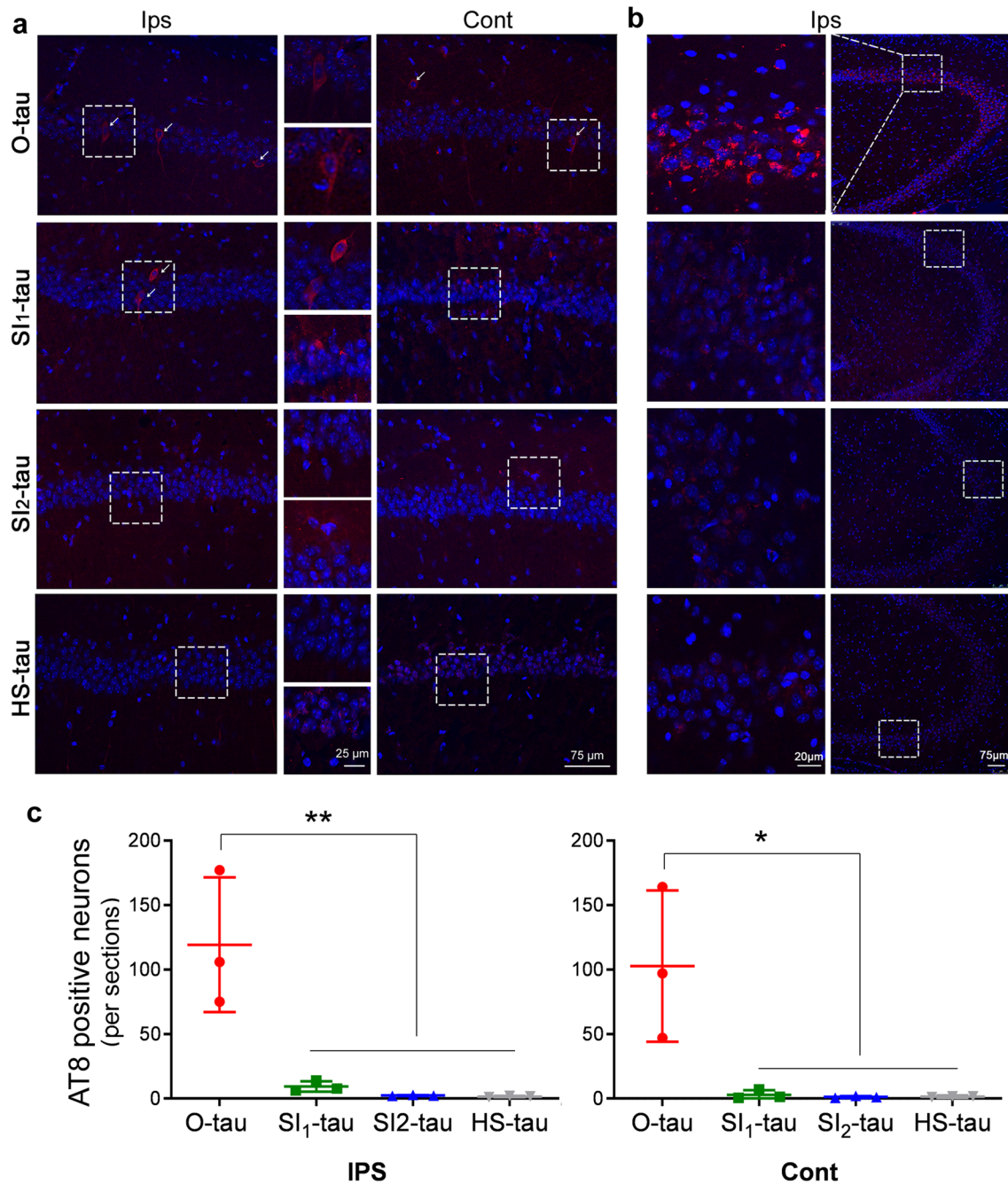


Fig. 8 AD tau fractions induce tau pathology differentially in vivo. **a, b** AD tau fractions at similar tau levels were injected into hippocampus of 18-month-old-FVB mice. Brain sections were immunostained with AT8 3 months after injection. Hoechst dye was used to stain nuclei. Representative AT8 immunostaining of ipsilateral (Ips) and contralateral (Cont) CA1s (**a**) and Ips CA3 (**b**) of the mouse hippocampus after injection with AD tau fractions. **c** AT8-positive neurons in Ips hippocampus (left) and Cont hippocampus (right) were quantified. Data are presented as mean \pm SD, ** $P < 0.05$; *** $P < 0.01$

O-tau yielded from 27,000 \times g to 235,000 \times g fraction of AD brain homogenate [39]. Different from the tau in the 235,000 \times g supernatant, O-tau was abnormally hyperphosphorylated and formed SDS- and

β -ME-resistant HMW aggregates, which lacked the N-terminal portion. O-tau displayed very potent prion-like activities, capturing/sequestering tau and seeding tau aggregation in cultured cells and in vivo. Heat

treatment removes aggregated tau from the supernatant [48]. We found that heat treatment did not change O-tau ability to capture tau. However, HS-tau derived from Sup-tau could not capture tau, suggesting that aggregated tau, but not monomeric tau has prion-like activity. It was reported that tau trimers are the minimal propagation unit spontaneously internalized to seed intracellular aggregation [44]. However, large (>10 mer) aggregated tau, but not small, oligomeric (<6 mer) tau, from P301S transgenic mouse brains seeded cellular tau aggregation [34]. Similarly, we previously found that compared with O-tau from AD brain, O-tau from 3xTg-AD mouse brain showed much weaker seeding activity [40]. Furthermore, tau monomer purified from AD brain also had intrinsic seeding activity, and self-associated to produce larger seed-competent assemblies. It was proposed that tau monomer occupies two distinct and stable conformational ensembles: inert and seeding-competent [45]. Thus, we speculate that the 235,000×g supernatant contains small aggregates or/and seeding-competent tau monomer that may not be SDS- and β-ME-resistant but could capture tau and heat-treatment removes both species of tau.

Similarly, serial sedimentation can divide tau from AD brain into various fractions [53]. It was found that 3,000×g and 10,000×g AD brain extracts, which presumably contained HMW proteins, could be up-taken by cultured neurons, but 50,000×g and 150,000×g extracts, from which HMW tau was depleted by sedimentation, could not be up-taken by neurons [53]. The 3,000×g brain extracts showed significantly higher seeding activity than 150,000×g extracts. Thus, the 3,000×g and 10,000×g extracts contain various sizes of oligomeric tau [53], which may serve as predominant seeds to template tau aggregation. Consistently, we found here that O-tau from 27,000×g to 235,000×g displayed the prion-like activities.

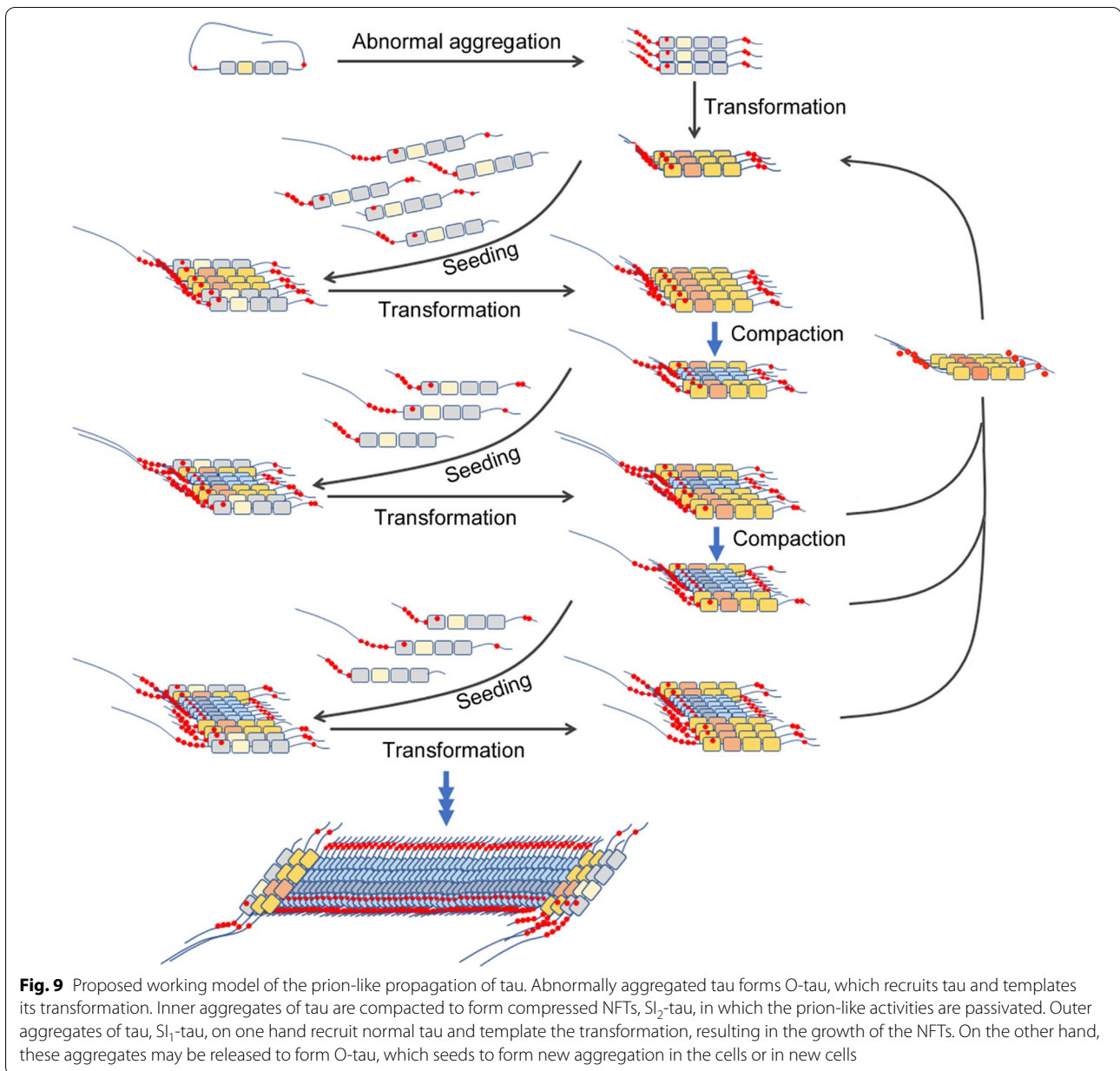
A previous study showed that AD tau from the 10,000×g brain homogenate in 0.1% sarkosyl-high salt buffer to 235,000×g in 1% sarkosyl induced tau aggregation in vitro and in vivo [28]. Different from this protocol, we first separated monomeric and oligomeric tau from aggregated tau by centrifugation of brain homogenate at 27,000×g and then incubated the pellet in the buffer containing 0.1% sarkosyl and centrifuged at 10,000×g. The supernatant and the pellet probably contain loose and compressed tau aggregates, respectively. These fractions were incubated in 1% sarkosyl containing buffer and centrifuged at 100,000×g to yield SI₁-tau and SI₂-tau. Both SI₁ and SI₂ fractions contained SDS- and β-ME-resistant HMW-tau, which did not react with N-terminal tau antibodies and was hyperphosphorylated at multiple sites. A relatively higher level of tau was detected in the

SI₁ fraction by the N-terminal antibodies than in the SI₂ fraction. Compared to O-tau, less tau was detected by the antibodies against microtubule-binding repeats, suggesting that SI₁-tau and SI₂-tau may be less accessible to these antibodies. Misfolded protein aggregates are usually resistant to proteolysis. We found that the resistance of O-tau, SI₁-tau, and SI₂-tau to proteinase K digestion was increased. Most interestingly, SI₁-tau was able to capture tau and to seed tau aggregation in cultured cells in prion-like fashion, but SI₂-tau was inert in these prion-like properties.

Prion-like spread of misfolded tau aggregates might underlie the stereotypic progression of neurodegenerative tauopathies. We reported in 1994 that the cytosolic and hyperphosphorylated tau from AD brain, named AD p-tau, sequestered tau and induced tau aggregation in vitro, which is the first study showing the prion-like activity of AD p-tau [3, 4]. AD p-tau was further purified by ion-exchange chromatography to remove non-hyperphosphorylated tau in O-tau [39]. Different from AD p-tau, PHF-tau could not sequester normal tau [4]. In the present study, we found that O-tau and SI₁-tau, but not SI₂-tau, captured tau and templated tau aggregation. We speculate that the major component of SI₂-tau may be PHF-tau.

Tau pathology initiates in the subcortical regions, transentorhinal cortex, and entorhinal cortex (stages I and II), then appears in the hippocampal formation and some parts of the neocortex (stages III and IV), followed by most of the neocortex (stages V and VI) [7, 10]. Immunohistochemical (IHC) study with AT8, a principal tool to define AD intraneuronal pathology [43], showed that AT8 signal first appears in the locus coeruleus (LC), suggesting that tau aggregation in the LC may represent the earliest phase of AD pathogenesis [9, 11]. Individuals at stages I and II are asymptomatic, but over half of the subjects at NFT stages III–IV exhibited signs of mild cognitive impairment, and over 90% of subjects at NFT stages V–VI showed moderate to severe dementia [31]. By using HEK293-tau-biosensor cells, tau-seeding activity from AD brains correlates positively with Braak stage and negatively with MMSE [19], but pathological seeding activity begins in the transentorhinal/entorhinal cortices (TRE/EC) rather than in the LC [36]. In the present study, we analyzed various tau fractions isolated from AD cerebral cortex at NFT stages V–VI and found that various AD tau fractions displayed different biochemical and prion-like properties, indicating the heterogeneity of pathological activity of tau fractions in AD brains.

In addition to AD, aggregated tau is a common feature of tauopathies. Distinct tau fractions from various tauopathies have been shown to induce distinct tau aggregation in mouse brains [50]. Thus, heterogeneity



of tau pathology both within AD and among different tauopathies could be due to different fractions with different biological and prion-like properties. This heterogeneity poses a major challenge in targeting tau for development of effective therapeutic treatment for tauopathies.

Taken together, we propose a working model of tau propagation (Fig. 9) in which O-tau recruits normal tau and templates the recruited tau and transforms to β -sheet conformation, resulting in loose aggregates, which recruit and template normal tau transformation. During the progression of tau pathogenesis, inner aggregated tau

is truncated and condensed to form compressed aggregates, resulting in loss of its prion-like activities. Based on this model, we speculate that O-tau may initiate tau aggregation, but SI_1 -tau may contribute to the growth of aggregated tau.

Acknowledgements

We are thankful to Dr. Peter Davies for his generous gift of tau monoclonal antibody PHF-1 and to Dr. Lester I. Binder for Tau-1 and to Ms. Maureen Marlow for copy-editing the manuscript. This work was supported in part by funds from the New York State Office for People With Developmental Disabilities, Nantong University, and the Neural Regeneration Co-innovation Center of Jiangsu Province and by grants from the U.S. Alzheimer's Association (DSAD-15-363172) and the Postgraduate Research & Practice Innovation Program of Jiangsu Province (KYCX18_2413).

Authors' contributions

L.L., R.S., J.G., Y.C.T., N.J., K.D., and J.X. carried out the study in vitro and in cultured cells. L.L., Y.Z., D.Z., R.W., and N.J. treated the animals and performed immunohistochemical studies. D.C., C.X.G., and K.I. helped in discussing the data and editing the paper. F.L. conceived, designed, and supervised the study and wrote the paper.

Availability of data and materials

The datasets generated and/or analyzed during the present study are available from the corresponding author, Dr. Fei Liu, upon reasonable request.

Ethics approval and consent to participate

All procedures involving mice were reviewed and approved by our Institutional Animal Care and Use Committee and were carried out according to guidelines of the National Institutes of Health. The use of autopsied frozen human brain tissue was in accordance with the National Institutes of Health guidelines and was exempted by the Institutional Review Board (IRB) of the New York State Institute for Basic Research in Developmental Disabilities because "the research does not involve intervention or interaction with the individuals" nor "is the information individually identifiable".

Competing interests

The authors declare that they have no competing interests.

Author details

¹ Department of Neurochemistry, Inge Grundke-Iqbal Research Floor, New York State Institute for Basic Research in Developmental Disabilities, 1050 Forest Hill Road, Staten Island, NY 10314, USA. ² Key Laboratory of Neuroregeneration of Jiangsu and Ministry of Education of China, Co-Innovation Center of Neuroregeneration, 19 Qixiu Road, Nantong 226001, Jiangsu, China.

Received: 3 February 2021 Accepted: 4 February 2021

Published online: 17 February 2021

References

- Ahmed Z, Cooper J, Murray TK, Garn K, McNaughton E, Clarke H, Parhizkar S, Ward MA, Cavallini A, Jackson S, Bose S, Clavaguera F, Tolnay M, Lavenir I, Goedert M, Hutton ML, O'Neill MJ (2014) A novel in vivo model of tau propagation with rapid and progressive neurofibrillary tangle pathology: the pattern of spread is determined by connectivity, not proximity. *Acta Neuropathol* 127(5):667–683
- Alafuzoff I, Adolfsson R, Grundke-Iqbal I, Winblad B (1987) Blood-brain barrier in Alzheimer dementia and in non-demented elderly. An immunocytochemical study *Acta Neuropathol* 73(2):160–166
- Alonso AC, Zaidi T, Grundke-Iqbal I, Iqbal K (1994) Role of abnormally phosphorylated tau in the breakdown of microtubules in Alzheimer disease. *Proc Natl Acad Sci U S A* 91(12):5562–5566
- Alonso AD, Grundke-Iqbal I, Iqbal K (1996) Alzheimer's disease hyperphosphorylated tau sequesters normal tau into tangles of filaments and disassembles microtubules. *Nat Med* 2(7):783–787
- Arriagada PV, Growdon JH, Hedley-Whyte ET, Hyman BT (1992) Neurofibrillary tangles but not senile plaques parallel duration and severity of Alzheimer's disease. *Neurology* 42(3 Pt 1):631–639
- Boluda S, Iba M, Zhang B, Raible KM, Lee VM, Trojanowski JQ (2015) Differential induction and spread of tau pathology in young PS19 tau transgenic mice following intracerebral injections of pathological tau from Alzheimer's disease or corticobasal degeneration brains. *Acta Neuropathol* 129(2):221–237
- Braak H, Braak E (1991) Neuropathological staging of Alzheimer-related changes. *Acta Neuropathol (Berl)* 82(4):239–259
- Braak H, Braak E (1995) Staging of Alzheimer's disease-related neurofibrillary changes. *Neurobiol Aging* 16(3):271–278 (discussion 278–284)
- Braak H, Del Tredici K (2011) The pathological process underlying Alzheimer's disease in individuals under thirty. *Acta Neuropathol* 121(2):171–181
- Braak H, Del Tredici K (2011) Alzheimer's pathogenesis: is there neuron-to-neuron propagation? *Acta Neuropathol* 121(5):589–595
- Braak H, Thal DR, Ghebremedhin E, Del Tredici K (2011) Stages of the pathologic process in Alzheimer disease: age categories from 1 to 100 years. *J Neuropathol Exp Neurol* 70(11):960–969
- Braak H, Feldengut S, Del Tredici K (2013) Pathogenesis and prevention of Alzheimer's disease: when and in what way does the pathological process begin? *Der Nervenarzt* 84(4):477–482
- Clavaguera F, Bolmont T, Crowther RA, Abramowski D, Frank S, Probst A, Fraser G, Stalder AK, Beibel M, Staufenbiel M, Jucker M, Goedert M, Tolnay M (2009) Transmission and spreading of tauopathy in transgenic mouse brain. *Nat Cell Biol* 11(7):909–913
- Clavaguera F, Akatsu H, Fraser G, Crowther RA, Frank S, Hench J, Probst A, Winkler DT, Reichwald J, Staufenbiel M, Ghetti B, Goedert M, Tolnay M (2013) Brain homogenates from human tauopathies induce tau inclusions in mouse brain. *Proc Natl Acad Sci U S A* 110(23):9535–9540
- de Calignon A, Polydoro M, Suarez-Calvet M, William C, Adamowicz DH, Kopeikina KJ, Pittstick R, Sahara N, Ashe KH, Carlson GA, Spire-Jones TL, Hyman BT (2012) Propagation of tau pathology in a model of early Alzheimer's disease. *Neuron* 73(4):685–697
- Dujardin S, Begard S, Caillierez R, Lachaud C, Delattre L, Carrier S, Loyens A, Galas MC, Bousset L, Melki R, Auregan G, Hantraye P, Brouillet E, Buee L, Colin M (2014) Ectosomes: a new mechanism for non-exosomal secretion of tau protein. *PLoS ONE* 9(6):e100760
- Fellous A, Francon J, Lennon AM, Nunez J (1977) Microtubule assembly in vitro. Purification of assembly-promoting factors. *Eur J Biochem* 78(1):167–174
- Frost B, Jacks RL, Diamond MI (2009) Propagation of tau misfolding from the outside to the inside of a cell. *J Biol Chem* 284(19):12845–12852
- Furman JL, Vaquer-Alicea J, White CL 3rd, Cairns NJ, Nelson PT, Diamond MI (2017) Widespread tau seeding activity at early Braak stages. *Acta Neuropathol* 133(1):91–100
- Goedert M, Clavaguera F, Tolnay M (2010) The propagation of prion-like protein inclusions in neurodegenerative diseases. *Trends Neurosci* 33(7):317–325
- Gong CX, Grundke-Iqbal I, Iqbal K (1994) Dephosphorylation of Alzheimer's disease abnormally phosphorylated tau by protein phosphatase-2A. *Neuroscience* 61(4):765–772
- Greenberg SG, Davies P (1990) A preparation of Alzheimer paired helical filaments that displays distinct tau proteins by polyacrylamide gel electrophoresis. *Proc Natl Acad Sci U S A* 87(15):5827–5831
- Grober E, Dickson D, Sliwinski MJ, Buschke H, Katz M, Crystal H, Lipton RB (1999) Memory and mental status correlates of modified Braak staging. *Neurobiol Aging* 20(6):573–579
- Grundke-Iqbal I, Iqbal K, Quinlan M, Tung YC, Zaidi MS, Wisniewski HM (1986) Microtubule-associated protein tau. A component of Alzheimer paired helical filaments. *J Biol Chem* 261(13):6084–6089
- Grundke-Iqbal I, Iqbal K, Tung YC, Quinlan M, Wisniewski HM, Binder LI (1986) Abnormal phosphorylation of the microtubule-associated protein tau (tau) in Alzheimer cytoskeletal pathology. *Proc Natl Acad Sci USA* 83(13):4913–4917
- Gu J, Xu W, Jin N, Li L, Zhou Y, Chu D, Gong CX, Iqbal K, Liu F (2020) Truncation of tau selectively facilitates its pathological activities. *J Biol Chem* 295(40):13812–13828
- Guo JL, Lee VM (2011) Seeding of normal Tau by pathological Tau conformers drives pathogenesis of Alzheimer-like tangles. *J Biol Chem* 286(17):15317–15331
- Guo JL, Narasimhan S, Changolkar L, He Z, Stieber A, Zhang B, Gathagan RJ, Iba M, McBride JD, Trojanowski JQ, Lee VM (2016) Unique pathological tau conformers from Alzheimer's brains transmit tau pathology in nontransgenic mice. *J Exp Med* 213(12):2635–2654
- Holmes BB, Furman JL, Mahan TE, Yamasaki TR, Mirbaha H, Eades WC, Belaygorod L, Cairns NJ, Holtzman DM, Diamond MI (2014) Proteopathic tau seeding predicts tauopathy in vivo. *Proc Natl Acad Sci U S A* 111(41):E4376–E4385
- Hu W, Zhang X, Tung YC, Xie S, Liu F, Iqbal K (2016) Hyperphosphorylation determines both the spread and the morphology of tau pathology. *Alzheimers Dement* 12(10):1066–1077
- Hyman BT, Phelps CH, Beach TG, Bigio EH, Cairns NJ, Carrillo MC, Dickson DW, Duyckaerts C, Frosch MP, Masliah E, Mirra SS, Nelson PT, Schneider JA, Thal DR, Thies B, Trojanowski JQ, Vinters HV, Montine TJ (2012) National Institute on Aging-Alzheimer's Association guidelines for the

- neuropathologic assessment of Alzheimer's disease. *Alzheimers Dement* 8(1):1–13
32. Iba M, Guo JL, McBride JD, Zhang B, Trojanowski JQ, Lee VM (2013) Synthetic tau fibrils mediate transmission of neurofibrillary tangles in a transgenic mouse model of Alzheimer's-like tauopathy. *J Neurosci* 33(3):1024–1037
 33. Iqbal K, Liu F, Gong CX (2016) Tau and neurodegenerative disease: the story so far. *Nat Rev Neurol* 12(1):15–27
 34. Jackson SJ, Kerridge C, Cooper J, Cavallini A, Falcon B, Cella CV, Landi A, Szekeres PG, Murray TK, Ahmed Z, Goedert M, Hutton M, O'Neill MJ, Bose S (2016) Short Fibrils Constitute the Major Species of Seed-Competent Tau in the Brains of Mice Transgenic for Human P301S Tau. *J Neurosci* 36(3):762–772
 35. Johnson KA, Schultz A, Betensky RA, Becker JA, Sepulcre J, Rentz D, Mormino E, Chhatwal J, Amariglio R, Papp K, Marshall G, Albers M, Mauro S, Pepin L, Alverio J, Judge K, Philiostaint M, Shoup T, Yokell D, Dickerson B, Gomez-Isla T, Hyman B, Vasdev N, Sperling R (2016) Tau positron emission tomographic imaging in aging and early Alzheimer disease. *Ann Neurol* 79(1):110–119
 36. Kaufman SK, Del Tredici K, Thomas TL, Braak H, Diamond MI (2018) Tau seeding activity begins in the transentorhinal/entorhinal regions and anticipates phospho-tau pathology in Alzheimer's disease and PART. *Acta Neuropathol* 136(1):57–67
 37. Kfoury N, Holmes BB, Jiang H, Holtzman DM, Diamond MI (2012) Transcellular propagation of Tau aggregation by fibrillar species. *J Biol Chem* 287(23):19440–19451
 38. Khatoun S, Grundke-Iqbal I, Iqbal K (1992) Brain levels of microtubule-associated protein tau are elevated in Alzheimer's disease: a radio-immuno-slot-blot assay for nanograms of the protein. *J Neurochem* 59(2):750–753
 39. Kopke E, Tung YC, Shaikh S, Alonso AC, Iqbal K, Grundke-Iqbal I (1993) Microtubule-associated protein tau. Abnormal phosphorylation of a non-paired helical filament pool in Alzheimer disease. *J Biol Chem* 268(32):24374–24384
 40. Li L, Jiang Y, Hu W, Tung YC, Dai C, Chu D, Gong CX, Iqbal K, Liu F (2019) Pathological Alterations of Tau in Alzheimer's Disease and 3xTg-AD Mouse Brains. *Mol Neurobiol* 56(9):6168–6183
 41. Liu F, Shi J, Tanimukai H, Gu J, Grundke-Iqbal I, Iqbal K, Gong CX (2009) Reduced O-GlcNAcylation links lower brain glucose metabolism and tau pathology in Alzheimer's disease. *Brain* 132(Pt 7):1820–1832
 42. Liu L, Drouet V, Wu JW, Witter MP, Small SA, Clelland C, Duff K (2012) Transynaptic spread of tau pathology in vivo. *PLoS ONE* 7(2):e31302
 43. Mercken M, Vandermeeren M, Lubke U, Six J, Boons J, Van de Voorde A, Martin JJ, Gheuens J (1992) Monoclonal antibodies with selective specificity for Alzheimer Tau are directed against phosphatase-sensitive epitopes. *Acta Neuropathol* 84(3):265–272
 44. Mirbaha H, Holmes BB, Sanders DW, Bieschke J, Diamond MI (2015) Tau trimers are the minimal propagation unit spontaneously internalized to seed intracellular aggregation. *J Biol Chem* 290(24):14893–14903
 45. Mirbaha H, Chen D, Morazova OA, Ruff KM, Sharma AM, Liu X, Goodarzi M, Pappu RV, Colby DW, Mirzaei H, Joachimiak LA, Diamond MI (2018) Inert and seed-competent tau monomers suggest structural origins of aggregation. *Elife* 7:e36584
 46. Novak M, Kabat J, Wischik CM (1993) Molecular characterization of the minimal protease resistant tau unit of the Alzheimer's disease paired helical filament. *EMBO J* 12(1):365–370
 47. Peeraer E, Bittelbergs A, Van Kolen K, Stancu IC, Vasconcelos B, Mahieu M, Duytschaever H, Ver Donck L, Torremans A, Sluydts E, Van Acker N, Kemp JA, Mercken M, Brunden KR, Trojanowski JQ, Dewachter I, Lee VM, Moechars D (2015) Intracerebral injection of preformed synthetic tau fibrils initiates widespread tauopathy and neuronal loss in the brains of tau transgenic mice. *Neurobiol Dis* 73:83–95
 48. Planel E, Tatebayashi Y, Miyasaka T, Liu L, Wang L, Herman M, Yu WH, Luchsinger JA, Wadzinski B, Duff KE, Takashima A (2007) Insulin dysfunction induces in vivo tau hyperphosphorylation through distinct mechanisms. *J Neurosci* 27(50):13635–13648
 49. Quinn JP, Corbett NJ, Kellett KAB, Hooper NM (2018) Tau Proteolysis in the Pathogenesis of Tauopathies: Neurotoxic Fragments and Novel Biomarkers. *J Alzheimers Dis* 63(1):13–33
 50. Sanders DW, Kaufman SK, DeVos SL, Sharma AM, Mirbaha H, Li A, Barker SJ, Foley AC, Thorpe JR, Serpell LC, Miller TM, Grinberg LT, Seeley WW, Diamond MI (2014) Distinct tau prion strains propagate in cells and mice and define different tauopathies. *Neuron* 82(6):1271–1288
 51. Scholl M, Lockhart SN, Schonhaut DR, O'Neil JP, Janabi M, Ossenkoppele R, Baker SL, Vogel JW, Faria J, Schwimmer HD, Rabinovici GD, Jagust WJ (2016) PET Imaging of Tau Deposition in the Aging Human Brain. *Neuron* 89(5):971–982
 52. Schwarz AJ, Yu P, Miller BB, Shcherbinin S, Dickson J, Navitsky M, Joshi AD, Devous MD Sr, Mintun MS (2016) Regional profiles of the candidate tau PET ligand 18F-AV-1451 recapitulate key features of Braak histopathological stages. *Brain* 139(Pt 5):1539–1550
 53. Takeda S, Wegmann S, Cho H, DeVos SL, Commins C, Roe AD, Nicholls SB, Carlson GA, Pitstick R, Nobuhara CK, Costantino I, Frosch MP, Muller DJ, Irimia D, Hyman BT (2015) Neuronal uptake and propagation of a rare phosphorylated high-molecular-weight tau derived from Alzheimer's disease brain. *Nat Commun* 6:84–90
 54. Wang Y, Garg S, Mandelkow EM, Mandelkow E (2010) Proteolytic processing of tau. *Biochem Soc Trans* 38(4):955–961
 55. Wischik CM, Novak M, Edwards PC, Klug A, Tichelaar W, Crowther RA (1988) Structural characterization of the core of the paired helical filament of Alzheimer disease. *Proc Natl Acad Sci U S A* 85(13):4884–4888
 56. Wischik CM, Novak M, Thogersen HC, Edwards PC, Runswick MJ, Jakes R, Walker JE, Milstein C, Roth M, Klug A (1988) Isolation of a fragment of tau derived from the core of the paired helical filament of Alzheimer disease. *Proc Natl Acad Sci U S A* 85(12):4506–4510
 57. Yanamandra K, Kfoury N, Jiang H, Mahan TE, Ma S, Maloney SE, Wozniak DF, Diamond MI, Holtzman DM (2013) Anti-tau antibodies that block tau aggregate seeding in vitro markedly decrease pathology and improve cognition in vivo. *Neuron* 80(2):402–414
 58. Zilka N, Filipcik P, Koson P, Fialova L, Skrabana R, Zilkova M, Rolkova G, Kontsekova E, Novak M (2006) Truncated tau from sporadic Alzheimer's disease suffices to drive neurofibrillary degeneration in vivo. *FEBS Lett* 580(15):3582–3588

Publisher's Note

Springer Nature remains neutral with regard to jurisdictional claims in published maps and institutional affiliations.